ASTRONOMY & ASTROPHYSICS
SUPPLEMENT SERIES

Astron. Astrophys. Suppl. Ser. **115,** 219-226 (1996)

Photometric Bgr survey of the distant clusters of galaxies Cl 1613+3104 and Cl 1600+4109⋆,⋆⋆

R. Pelló[1,3] and R. Vílchez–Gómez[2]

[1] Laboratoire d'Astrophysique de Toulouse, Observatoire Midi–Pyrénées, 14 av. Édouard Belin, F-31400 Toulouse, France
[2] Departament d'Astronomia i Meteorologia, Universitat de Barcelona, Av. Diagonal 647, E-08028 Barcelona, Spain
[3] Laboratori d'Astrofísica del Institut d'Estudis Catalans, Barcelona, Spain

Received February 13, accepted July 7, 1995

Abstract. — We present a set of photometric data concerning two distant clusters of galaxies: Cl 1613+3104 ($z = 0.415$) and Cl 1600+4109 ($z = 0.540$). The photometric survey extends to a field of about $4' \times 3'$. It was performed in 3 filters: Johnson B, and Thuan–Gunn g and r. The sample includes 679 objects in the field of Cl 1613+3104 and 334 objects in Cl 1600+4109.

Key words: galaxies: clusters: individual: Cl 1613+3104 and Cl 1600+4109

1. Introduction

This paper gives the results obtained on the photometric survey of two distant clusters of galaxies: Cl 1613+3104 ($\alpha_{1950} = 16^h\ 13^m\ 48\overset{s}{.}0$; $\delta_{1950} = 31°\ 05'\ 00\overset{''}{.}0$; $z = 0.415$; Sandage et al. 1976) and Cl 1600+4109 ($\alpha_{1950} = 16^h\ 00^m\ 23\overset{s}{.}0$; $\delta_{1950} = 41°\ 09'\ 39\overset{''}{.}0$; $z = 0.540$; Henry et al. 1982). Cl 1613+3104 ($l = 50\overset{°}{.}58$, $b = +45\overset{°}{.}56$) is a very rich cluster of galaxies which shows X-ray (Henry et al. 1982) and radio emission (Jaffe 1982). Recently, Vílchez–Gómez et al. (1994) have reported the existence of a diffuse stellar component in this cluster. Cl 1600+4109 ($l = 65\overset{°}{.}21$, $b = +48\overset{°}{.}72$) belongs to the sample of Gunn et al. (1986) and its upper limit for the X-ray emission in the range 0.5–4.5 keV is 1.6 10^{44} erg s^{-1} (Henry et al. 1982). The present paper constitutes the database of a recent study by Vílchez–Gómez et al. (1995) on the galaxy content and structure of these two clusters.

2. Observations and data reduction

The survey presented here was performed in two different runs (May 1987 and July 1988) at the F/3.4 prime focus of the 3.5 m telescope of the *C.A.H.A* (Calar Alto, Almería, Spain). The detector used was an RCA CCD, with a pixel size of $0\overset{''}{.}506$. The equivalent field size of the CCD was about $4\overset{'}{.}4 \times 2\overset{'}{.}8$. The images were obtained under photometric conditions. The filters used were Johnson B and Thuan–Gunn g and r.

The photometric calibration was done using Johnson and Thuan–Gunn system standard stars from Kent (1985) and Thuan & Gunn (1976), and several standard stars in the globular cluster M 92 (Kent 1985, in g and r; Sandage & Walker 1966, in B). During the same nights and, in principle, under the same conditions, we have also obtained images on a comparison field near each cluster. These images were reduced in the same way as the cluster ones. They have been used to correct for the field contamination, as it is explained in Vílchez–Gómez et al. (1995).

Photometry of objects in these fields (cluster + comparison field) was obtained with the software package *Amaphot* developed at the *Observatoire Midi–Pyrénées* (Toulouse, France). This method is based on the automatic detection of objects and their subsequent fit by ellipses. A profile for each object is calculated through elliptical concentric rings, with the same ellipticity and orientation as the previously fitted ellipse. To obtain magnitudes, profiles are integrated down to a limiting isophote. For each object, colors are obtained through magnitudes which are calculated inside the elliptical aperture determined from the limiting isophote of a reference filter. The filter g has been taken as a reference in these catalogs to calculate the colors $B-g$ and $g-r$, as presented in Tables

Send offprint requests to: R. Pelló
⋆Based on observations made with the 3.5 m telescope of the Centro Astronómico Hispano-Alemán de Calar Alto in Almería (Spain)
⋆⋆Tables 2 and 3 are available in electronic form at the CDS via anonymous ftp 130.79.128.5

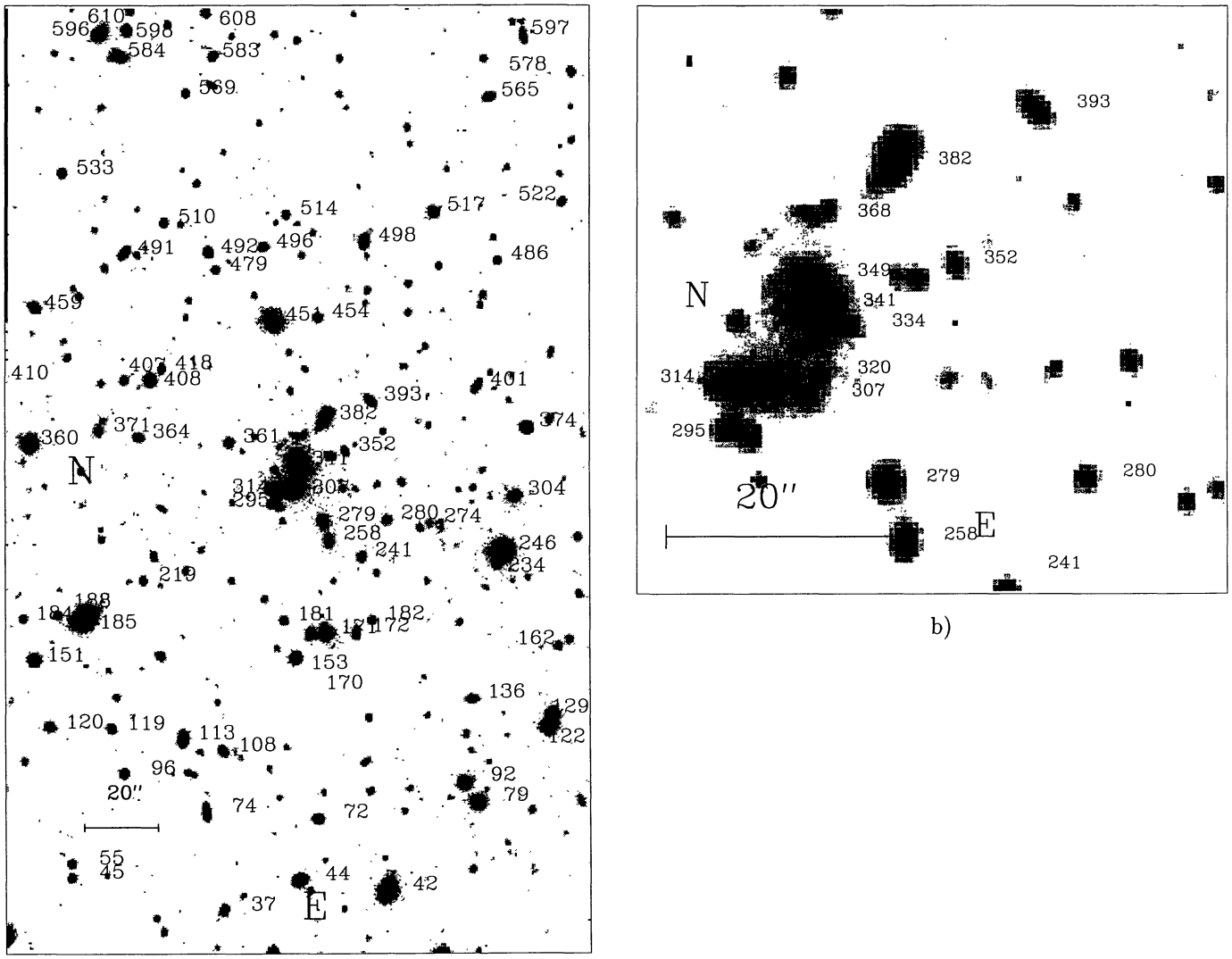

Fig. 1. a) r image of the cluster Cl 1613+3104 showing the identification numbers for objects brighter than $r = 22$. The exposure time was 1500 s. **b)** The central part of the cluster Cl 1613+3104 (same comments as in Fig. 1a)

2 and 3, and also to compute the value of $B - r$ which is used in Vílchez–Gómez et al. (1995).

Table 1 shows the summary of the main characteristics of the photometric CCD images. Columns 1 to 4 of this Table are self-explanatory. Columns 5 and 6 give, respectively, the completeness and the effective limits in magnitude. The detection thresholds given in Cols. 7 and 8 are the typical upper values of the surface brightness for the detection of an object at 1σ and 3σ of the sky noise. The effective limit in magnitude for a given image is defined as the faintest threshold in the magnitude distribution which contains 10% of the sample.

3. Results

3.1. *The catalog*

The catalogs of Cl 1613+3104 and Cl 1600+4109 are presented in Tables 2 and 3, respectively. The data given in the columns of these tables are, from left to right:

1. Identification number.
2. x coordinate in arcsec with respect to the central galaxy, increasing southward.
3. y coordinate in arcsec with respect to the central galaxy, increasing westward.
4. B (limiting isophote 27.0 mag arcsec^{-2} in Cl 1613+3104 and 27.5 mag arcsec^{-2} in Cl 1600+4109).

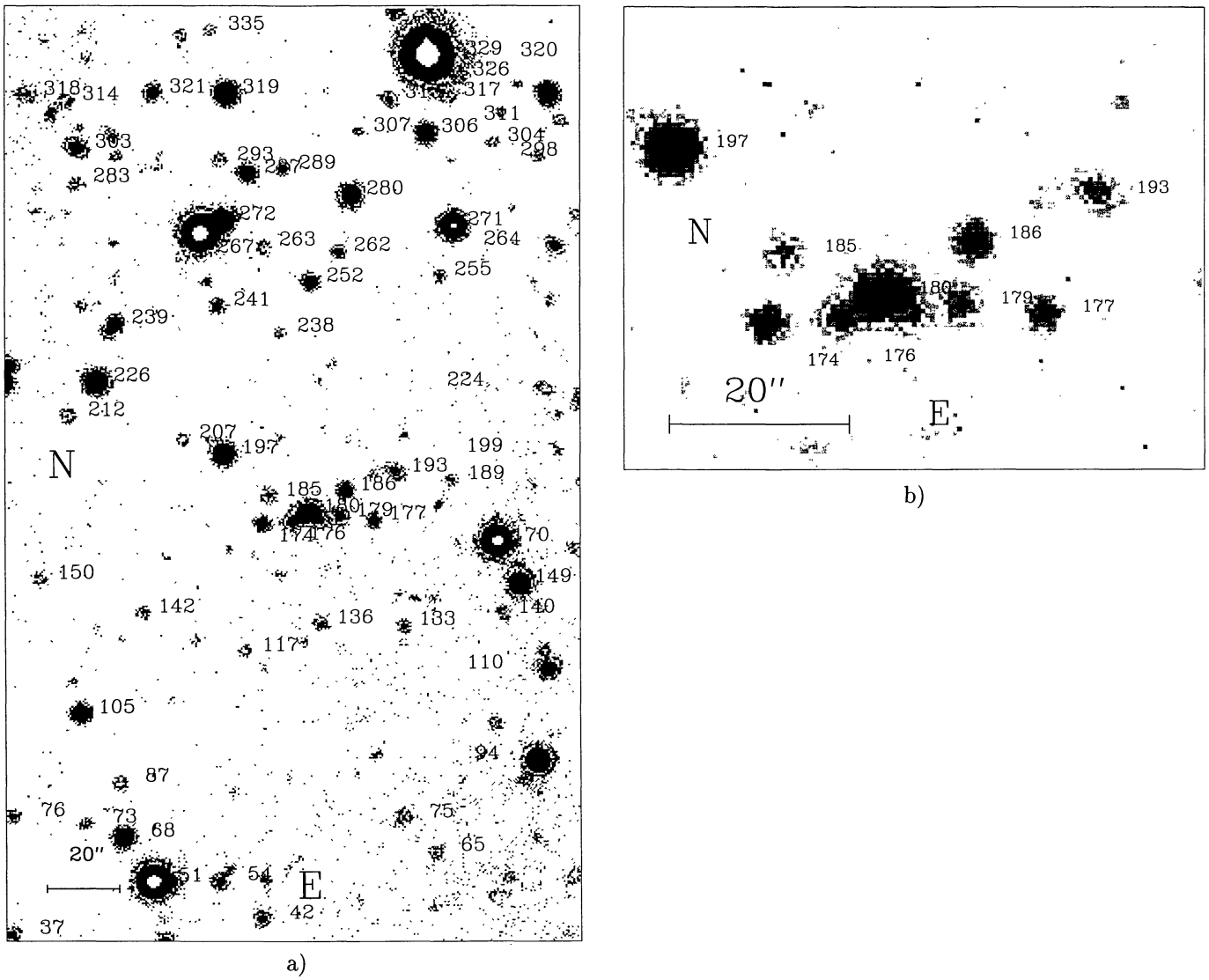

Fig. 2. a) r image of the cluster Cl 1600+4109 showing the identification numbers for objects brighter than $r = 23$. The exposure time was 2039 s. **b)** The central part of the cluster Cl 1600+4109 (same comments as in Fig. 2a)

5. g (limiting isophote 27.0 mag arcsec^{-2} in Cl 1613+3104 and 27.5 mag arcsec^{-2} in Cl 1600+4109).
6. r (limiting isophote 27.0 mag arcsec^{-2} in Cl 1613+3104 and 27.5 mag arcsec^{-2} in Cl 1600+4109).
7. $B - g$ (limiting isophote corresponds to g).
8. $g - r$ (limiting isophote corresponds to g).
9. Criterion to discriminate between stars and galaxies in B (see Sect. 3.3). Stars, galaxies and unclassified objects are identified respectively with 0, 2 and 1.
10. Same information as in Col. 9 for the g image.
11. Same information as in Col. 9 for the r filter. The mean value of $r1$ and $r2$ has been tabulated when the object is detected in both frames.
12. Final classification of objects as stars (0), galaxies (2) or ambiguous (1), according to the results in Col. 9 to 11. This is the criterion used in the paper by Vílchez–Gómez et al. (1995) (see Sect. 3.3). Saturated stars are identified by "s".

679 objects have been detected in the field of Cl 1613+3104, in at least one filter, 575 of which are located in a field of about $4' \times 3'$ around the center of the cluster. In an equivalent field size, only 334 objects have been found in Cl 1600+4109. In addition to the fact that Cl 1613+3104 is probably richer than Cl 1600+4109, there are two explanations for this difference: the redshift of Cl 1600+4109 is higher than that of Cl 1613+3104 and, in general, the images of the former have a worse seeing. This is the reason why we have taken a lower isophote to obtain the integrate magnitudes in the field of Cl 1600+4109. The number of objects detected in the comparison field of Cl 1613+3104 is 357 whereas there are only 192 objects in the comparison field of Cl 1600+4109. As the galactic

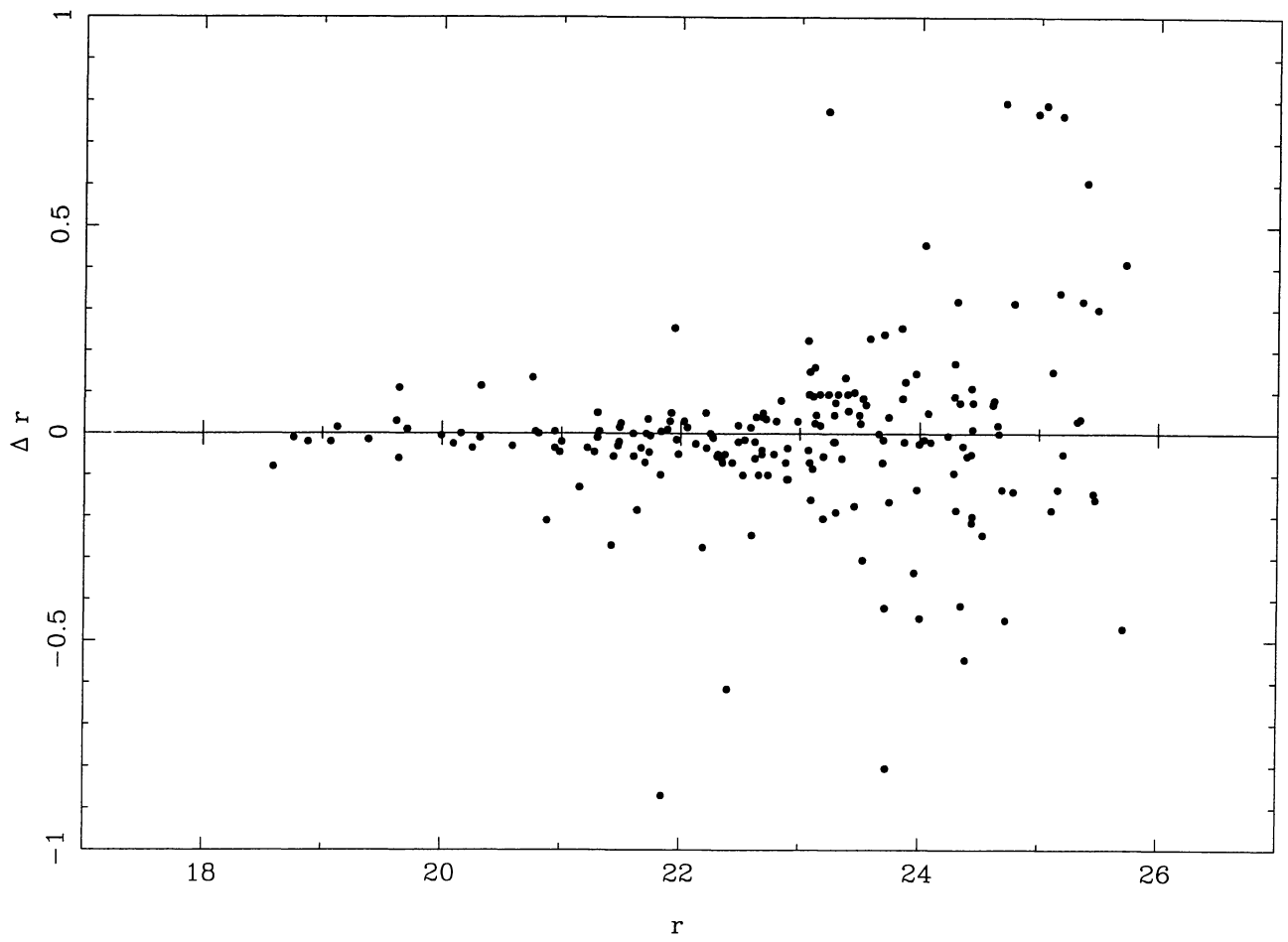

Fig. 3. Maximum value of the difference between the r magnitudes for the same object obtained in two different r frames of Cl 1613+3104, versus the mean r magnitude

coordinates of both clusters are similar, the difference is probably due to the seeing.

The identification charts of these clusters appear in Figs. 1 and 2. In order to avoid confusion, only objects brighter than $r = 22$ for Cl 1613+3104 and $r = 23$ for Cl 1600+4109 have been numbered.

3.2. *Photometric accuracy*

To estimate the photometric accuracy, we have taken the r images in both clusters. Magnitudes obtained in the different images for a given object have been used to determine a dispersion in the data as a function of the magnitude. Figures 3 and 4 illustrate these results, in the case of Cl 1613+3104 and Cl 1600+4109, respectively. The photometric accuracy is about 0.05 magnitudes for the brightest objects ($r \leq 20$), it is 0.1 for objects between $r = 20$ and $r = 23$, it is between 0.2 and 0.3 for objects between $r = 23$ and $r = 24$, and it increases rapidly to 0.5−0.7 for the faintest objects in the sample. It is worth noting that the dispersion given includes all the usual sources of error: the photometric calibration, the uncertainties related to sampling and/or seeing, as well as the internal errors associated to the method used by *Amaphot* to integrate magnitudes and the statistical scatter in the signal. Nevertheless, the results found by Le Borgne et al. (1992) using *Amaphot* on a set of images taken in the same photometric conditions, during the same night, with the same filters, CCD, seeing, sampling and exposure times (thus, equivalent frames), strongly suggest that internal errors are small compared to the other sources of error. In addition, objects identified as stars in these fields show colors compatible with the expected sequence for stars on the color-color plane.

3.3. *Discrimination between stars and galaxies*

Fore and background objects coincidental with the line-of-sight of these clusters have been corrected statistically, using the comparison fields. Nevertheless, it is relatively easy to obtain a criterion to discriminate between stars and galaxies in a large range of magnitude. As it is well known, the morphological differences between stars and galaxies tend to vanish at faint magnitudes and it is extremely

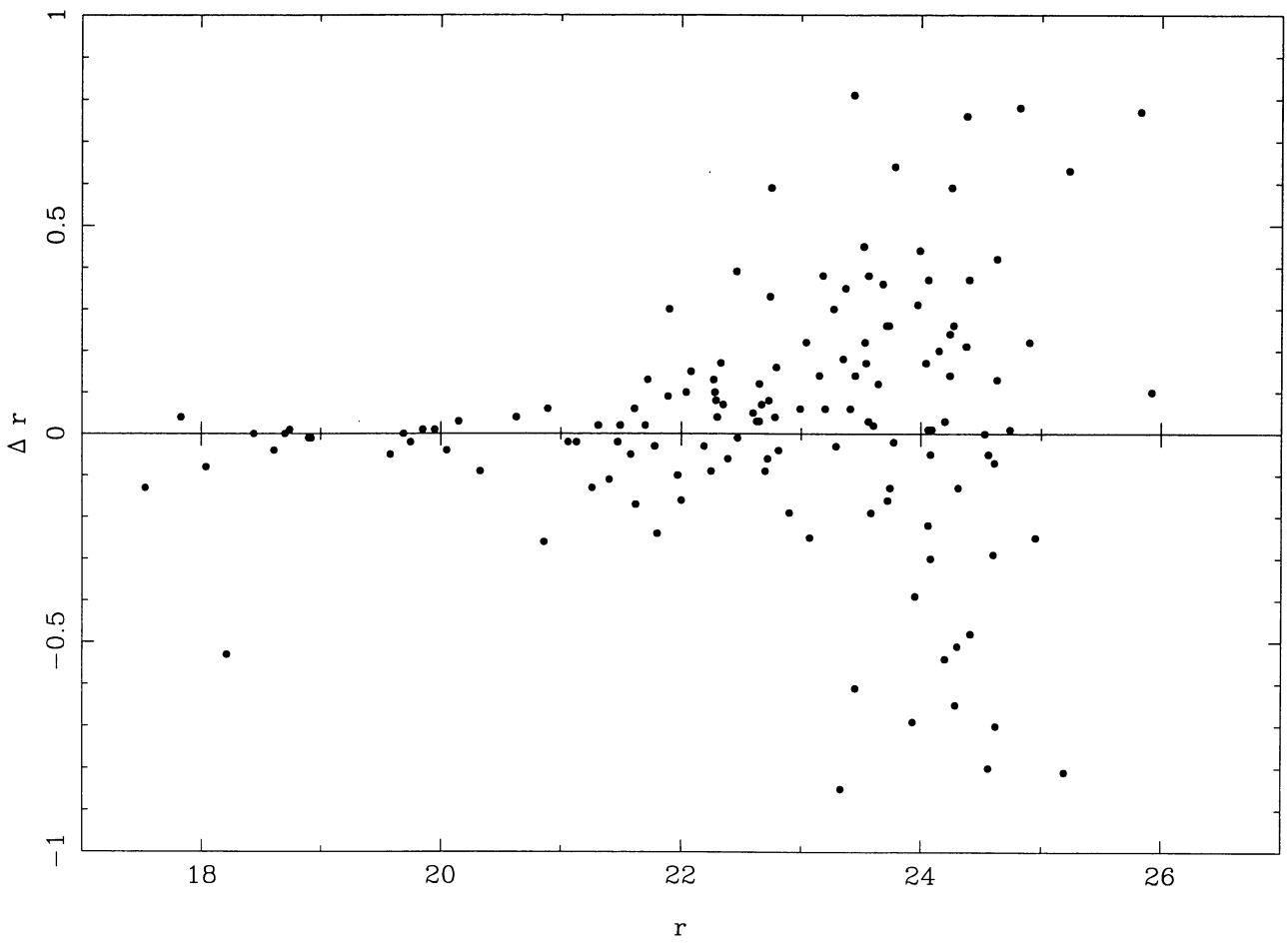

Fig. 4. The same as in Fig. 3 in the case of Cl 1600+4109

Table 1. Characteristics of the photometric CCD images

Date	Cluster	filter	seeing	magnitude of completeness	limiting magnitude	surface brightness detection limits		exposure time
						(1σ)	(3σ)	
			($''$)			(mag arcsec^{-2})		(s)
21 May 87	Cl 1613+3104	g	1.2	24.50	25.25	27.2	26.0	1800
21 May 87	cf* Cl 1613	g	1.8	24.25	25.50	27.7	26.5	1800
21 May 87	Cl 1613+3104	r	1.4	23.25	24.75	26.6	25.4	1500
21 May 87	Cl 1613+3104	r	1.1	24.25	25.00	26.8	25.6	1500
21 May 87	cf Cl 1613	r	1.8	24.00	25.50	27.8	26.6	1500
8 July 88	Cl 1613+3104	B	1.2	24.25	25.50	27.1	25.9	2700
9 July 88	cf Cl 1613	B	1.4	24.25	25.00	26.9	25.7	2700
24 May 87	Cl 1600+4109	g	1.8	24.50	25.50	27.3	26.1	2400
24 May 87	cf Cl 1600	g	2.2	24.50	24.75	27.2	26.0	2400
24 May 87	Cl 1600+4109	r	2.6	23.75	24.75	27.1	25.9	1800
24 May 87	Cl 1600+4109	r	2.3	23.75	25.00	27.2	26.0	2039
24 May 87	cf Cl 1600	r	2.8	23.75	24.50	27.2	26.0	2039
8 July 88	Cl 1600+4109	B	1.6	24.50	25.50	27.1	25.9	2700
9 July 88	cf Cl 1600	B	1.3	24.50	25.25	26.8	25.6	2700

* cf: comparison field

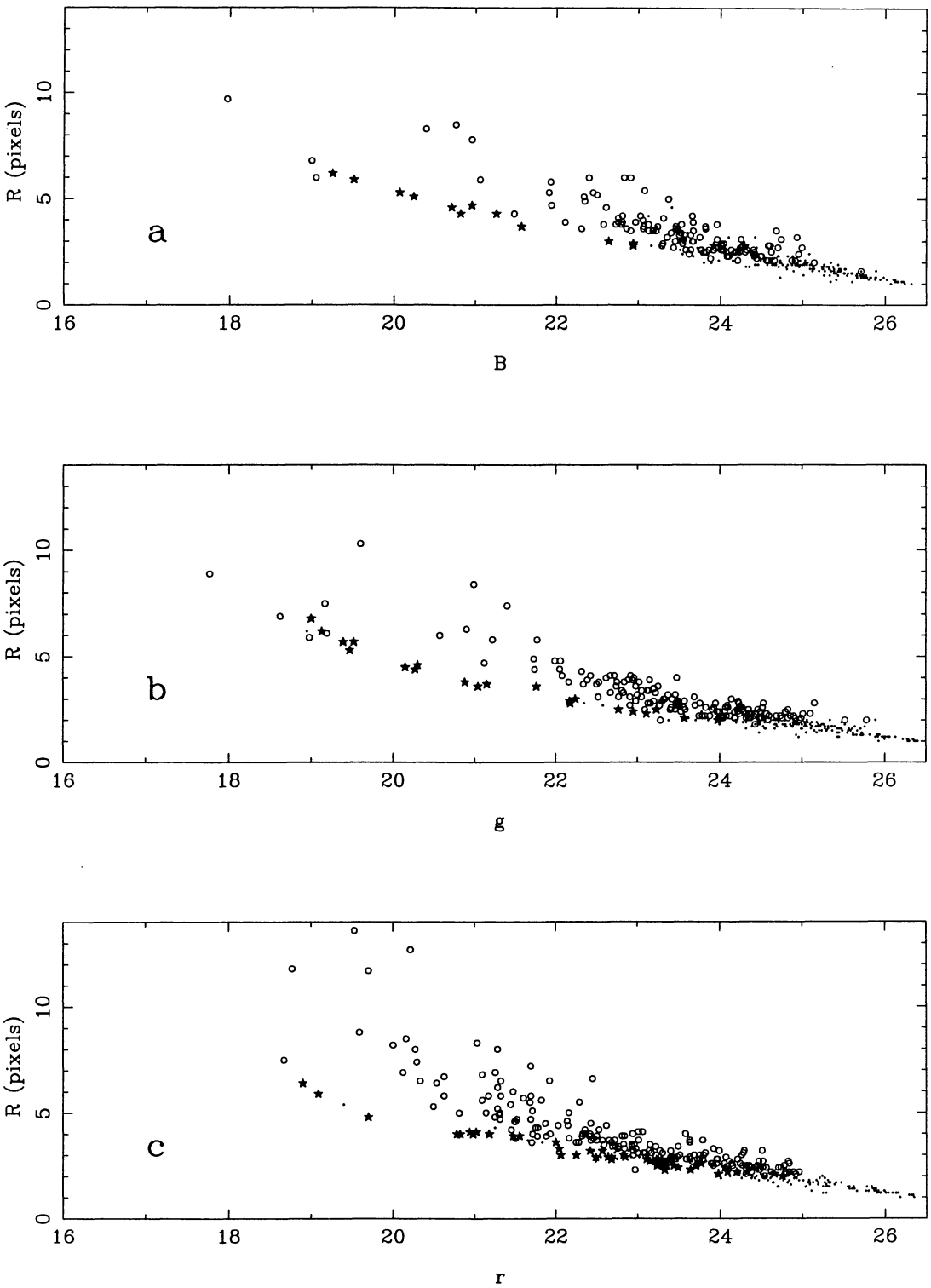

Fig. 5. Isophotal radii corresponding to 27 mag arcsec^{-2} versus magnitude in the field of Cl 1613+3104. Objects identified automatically as stars are shown as black stars, together with objects identified as galaxies (open circles) and unidentified objects (small dots): **a)** B, **b)** g and **c)** r. For objects brighter than $r = 21-22$, two separate sequences appear corresponding to stars (lower branch) and galaxies (upper branch)

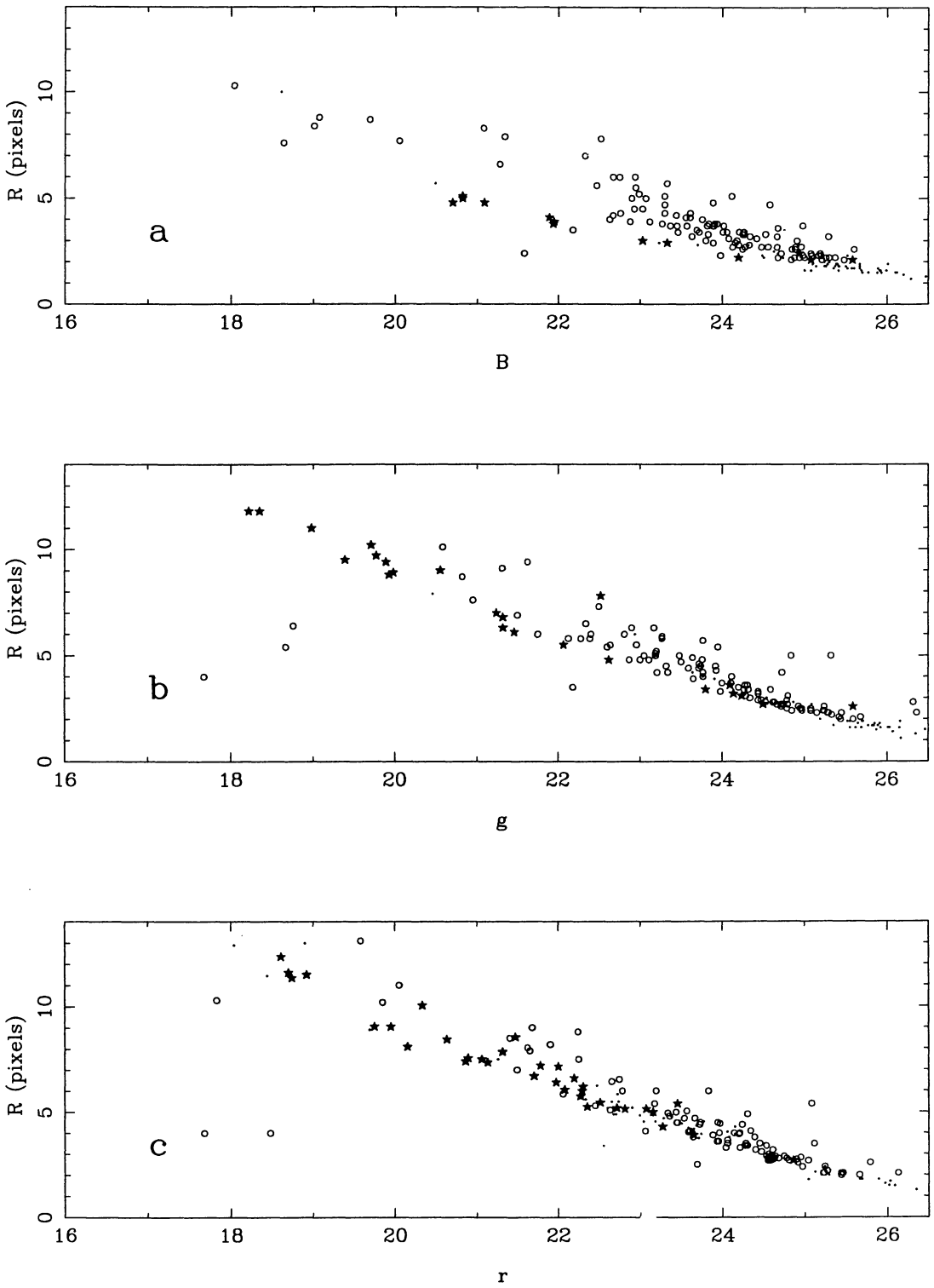

Fig. 6. The same as in Fig. 5 in the field of Cl 1600+4109. The effect of a seeing worse than 1.5 arcsec is clearly visible

difficult to distinguish between both populations. This effect is clearly shown by Molinari et al. (1990), among others. When the isophotal radii are plotted against magnitudes, two different sequences appear in the diagram, which correspond to two different populations of objects. As an example, we show this diagram in Fig. 5, in the case of Cl 1613+3104. For objects brighter than $r = 22$, there are two different sequences: the upper branch, which corresponds to galaxies, and the lower narrow branch of stars. Although the number of non-saturated bright stars in our fields is low, this is a general trend. Molinari et al. (1990) estimate that it is almost impossible to discriminate between stars and galaxies using this diagram for objects fainter than $r = 21$, with a pixel size of $0''.675$ and a seeing between $1''.3$ and $1''.4$. We have introduced a different method to improve this result, which is in good agreement with the precedent one for the brightest objects, and which is able to enlarge the range of discrimination in magnitude. For each object, a reduced χ^2 has been computed through the square of the difference between its sky-corrected profile and the observed normalized profile of a non-saturated reference star in the same frame. The probability that the observed profile yields a value of χ^2 at least as large as that observed if the profile corresponds to a stellar profile has been studied. When this probability exceeds 90%, we estimate that the object is a star, and it is identified by 0 in Tables 2 and 3. When the probability is smaller than 10%, the profile is clearly different from a stellar profile, and the object is classified as a galaxy (it is identified by 2 in the catalogue). In the intermediate case, there is no answer to the test and the object is unclassified. Objects of this kind are identified by 1 in the catalogue. As it is shown in Fig. 5, where the different kinds of objects have been displayed, the result of this test for objects brighter than $r = 21$ is the same as that obtained with the morphological criterion alone. Several saturated bright stars are misclassified, as expected in this case. The two populations of objects (stars and galaxies) separate from each other up to a magnitude $r \sim 23$. For objects fainter than this, the two populations merge and the separation becomes difficult. It is impossible to obtain a reliable separation for objects fainter than $r = 25$ (these objects are all unclassified). Besides, this method is very sensitive to the seeing and sampling. In our case, it is really hard to sepparate between stars and galaxies when the seeing is worse than 1.5 arcsec. This effect is shown in Fig. 6, where the same diagram as in Fig. 5 is presented, in the case of Cl 1600+4109. The final classification criterion used in the paper by Vílchez–Gómez et al. (1995) is given in Col. 12 of Tables 2 and 3. An object is classified as a star (0) or as a galaxy (2) when it has been identified unambiguously in at least one filter. An object with contradictory classifications or unclassified everywhere is listed as ambiguous (1). Objects showing contradictory classifications among the different filters represent less than 10% of the sample (the typical value is only a few percent).

Acknowledgements. We wish to thank the technical staff of the CAHA for his help during the photometric runs at the 3.5 m telescope. We appreciated the help of J.F. Le Borgne and B. Sanahuja during the observations and the data reduction. This work has been supported by the Spanish DGICYT program PB90-0448 of the *Ministerio de Educación y Ciencia*, and, partially, by the Human Capital and Mobility Programme (EU), under contract CHRX-CT92-0044.

References

Gunn J.E., Hoessel J.G., Oke J.B., 1982, ApJ 306, 30
Henry J.P., Soltan A., Briel U., Gunn J.E., 1982, ApJ 262, 1
Jaffe W., 1982, ApJ 262, 15
Kent S.M., 1985, PASP 97, 165
Le Borgne J.F., Pelló R., Sanahuja B., 1992, A&AS 95, 87
Molinari E., Buzzoni A., Chincarini G., 1990, MNRAS 246, 576
Sandage A., Walker M.F., 1966, ApJ 143, 313
Sandage A., Kristian J., Westphal J.A., 1976, ApJ 205,688
Thuan T.X., Gunn J.E., 1976, PASP 88, 543
Vílchez–Gómez R., Pelló R., Sanahuja B., 1994, A&A 283, 37
Vílchez–Gómez R., Pelló R., Sanahuja B., 1995, A&A (submitted)